Chinese Chemical Letters 35 (2024) 108757

Contents lists available at ScienceDirect

Chinese Chemical Letters

journal homepage: www.elsevier.com/locate/cclet

Solvent and guest-binding-controlled chiroptical inversion of molecular devices based on pseudo[1]catenane-type pillar[5]arene derivatives

Yongjun Lv[a,b,*], Chao Xiao[b,c], Jingyu Ma[b], Dayang Zhou[d], Wanhua Wu[b], Cheng Yang[b,*]

[a] College of Chemical Engineering, Sichuan University of Science & Engineering, Zigong 643000, China
[b] College of Chemistry, Sichuan University, Chengdu 610064, China
[c] Zhejiang NHU Pharmeceutical Co., Ltd., Shaoxing 312000, China
[d] Comprehensive Analysis Center, ISIR, Osaka University, Osaka 567-0047, Japan

ARTICLE INFO

Article history:
Received 11 May 2023
Revised 20 June 2023
Accepted 29 June 2023
Available online 30 June 2023

Keywords:
Pillar[5]arene
N,O,S-containg ring
Bicycles
Solvation
Chirality inversion

ABSTRACT

Four pillar[5]arene-based bicyclic compounds, so-called molecular universal joint (MUJ), were synthesized by incorporating a bisamide ring containing N, O, or S-heteroatom groups, which served as stimuli-responsive chiroptical molecular devices. The structure of MUJ was confirmed by ^{1}H NMR spectra and single-crystal X-ray diffraction analysis, and their planar-chiral enantiomers were successfully separated. Chiroptical inversion behaviors from *in* to *out* configurations triggered by temperature, solvent, and guest complexation were investigated by circular dichroism spectra. Chiroptical inversion could be realized in the presence of adiponitrile in certain solvents due to the solvation effects on the side ring and the threading of the guest into the pillar[5]arene cavity. However, the stronger self-included interactions between the cavity and the inside ring of certain MUJs led to inhibition of the switching.

© 2023 Published by Elsevier B.V. on behalf of Chinese Chemical Society and Institute of Materia Medica, Chinese Academy of Medical Sciences.

Induced chiroptical inversion of macrocyclic arenes has garnered considerable attention due to the significant role of chirality in supramolecular assemblies, artificial nanostructures, molecular machines/devices and bio-functional systems [1–3]. To achieve control over chiroptical inversion in a single macrocyclic arene, various external stimuli, such as temperature [4,5], solvent [6,7], light [8–10], pH [11,12], redox [13,14], and competitive guests [15–19], have been explored. Among the reported chiral devices, planar chirality-based chiroptical inversions are particular attractive [20–23]. Pillararenes, a class of macrocyclic arenes known for their facile synthesis, ease of modification, and versatile host-guest complexation, have garnered considerable interest [24–31]. Pillar[5]arene-based pseudo[1]catenane-type compounds have emerged as an ideal platform for chiral molecular devices, achieved by fusing a side ring onto one hydroquinone unit, which we term as a molecular universal joint (MUJ) due to its rotational mobility [32–35]. We have studied supramolecular behavior of various macrocyclic compounds [36] and revealed a series of chiroptical inversion behaviors of MUJs manipulated by temperature [37], pressure [38], solvent [39], redox [40], and cation [19]. Notably, the nature of the fused side rings could critically influence the chiroptical inversion properties. To further elucidate the control effect on the side rings in the inversion events, we designed and synthesized four new pseudo[1]catenane-type pillar[5]arene derivatives by incorporating an N, O, or S-atom in the side ring, which could yield a pair of enantiomers with the fused ring being able to roll in or out of the pillar[5]arene cavity.

The synthesis of pillar[5]arene-based MUJs, namely **MUJ1**, **MUJ2**, **MUJ3** and **MUJ4** (Scheme 1), was carried out using pillar[5]arene-dicarboxylic acid (**P5–2A**) [41] and corresponding diamine in $CHCl_3$, resulting in yields of 43%, 60%, 47% and 49%, respectively [42]. **P5–2A** has been previously reported to exhibit a high affinity towards alkyldiamine guests [43]. The resultant host-guest complexes are stabilized by robust electrostatic interactions between dicarboxylic units and diamino groups, as well as multiple host-guest interactions between the cavity and the linear alkyl chain.

The host-guest complexations between **P5–2A** and different diamines, including 1,8-diaminooctane, diethylenetriamine, 1,8-diamino-3,6-dioxaoctane and cystamine, were firstly examined by ^{1}H NMR spectra (Figs. S1-S4 in Supporting information). In all cases, proton signals of diamines exhibited broadening with significant upfield shifts, indicating the diamine chain was included in the cavity of pillar[5]arene and suffered a strong shielding effect

* Corresponding authors.
E-mail addresses: yongjunlv@qq.com (Y. Lv), yangchengyc@scu.edu.cn (C. Yang).

https://doi.org/10.1016/j.cclet.2023.108757
1001-8417/© 2023 Published by Elsevier B.V. on behalf of Chinese Chemical Society and Institute of Materia Medica, Chinese Academy of Medical Sciences.

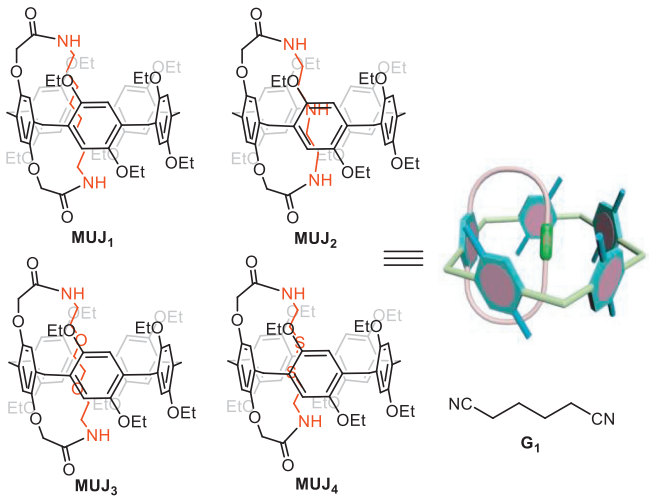

Scheme 1. Chemical structures of **MUJ1**, **MUJ2**, **MUJ3**, and **MUJ4**, guest **G1** and cartoon representation.

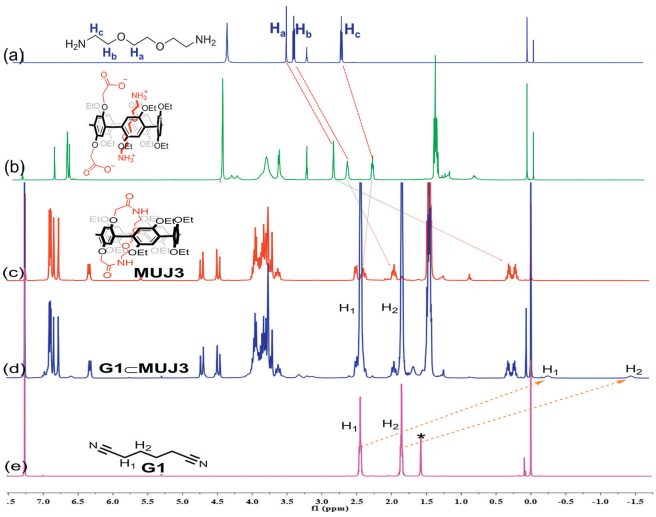

Fig. 1. ^{1}H NMR spectral (400 MHz, $CDCl_3$, 25 °C) of (a) diamine (0.08 mmol/L), (b) **P5–2A** (0.02 mmol/L) + diamine (0.04 mmol/L), (c) **MUJ3** (0.02 mmol/L), (d) **MUJ3** (0.02 mmol/L) + **G1** (10 μL, 4.00 equiv.), (d) **G1** (0.08 mmol/L).

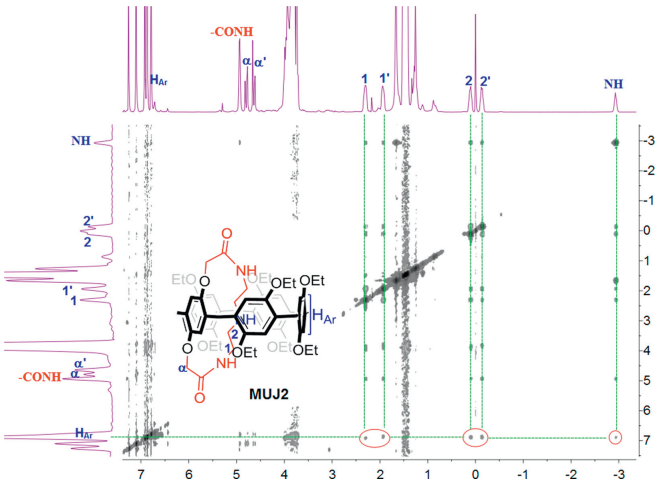

Fig. 2. ^{1}H-^{1}H NOESY NMR spectrum (400 MHz, $CDCl_3$, 25 °C) of **MUJ2**.

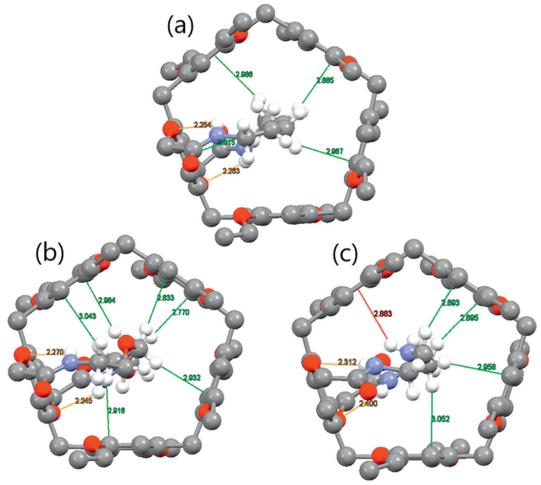

Fig. 3. Single crystal structure of (a) **MUJ1**, (b) **MUJ2**, and (c) **MUJ3**. Partial hydrogen atoms are omitted for clarity, oxygens are red, and nitrogens are blue. Orange, red, and green dashed lines indicate NH/O, NH/π, and CH/π interactions, respectively.

and led to a slow binding-release exchange on the NMR time scale, which unambiguously demonstrated the formation of a threaded complex between diamine chain and pillar[5]arene [44]. Moreover, MALDI-TOF-MS studies were carried out and confirmed a 1:1 stoichiometry of the host-guest complex (Fig. S5 in Supporting information). These results account for the synthesis process of desired compounds with host-guest intermediates.

MUJs were fully characterized by ^{1}H, ^{13}C NMR, and HR-MS spectra (Figs. S6 and S17 in Supporting information). Impressively, the proton signals of the side ring appeared significantly upfield because of the strong shielding effect of pillar[5]arene cavity in ^{1}H NMR. Moreover, peaks of methylene protons neighboring amide group split into two sets due to the side ring's blocked rolling, which results in different shielding effects on the two protons [45].

To further study their synthesis and inclusion properties, ^{1}H NMR experiments were carried out with relevant compounds in $CDCl_3$ (Fig. 1). Taking **MUJ3** for an example, the diamine first threaded into the cavity of **P5–2A** and formed [2]pseudorotaxane structure. As shown in Figs. 1a and b, all of the proton signals of diamine shifted upfield ($\Delta\delta = 0.70$ ppm for H_a, 0.78 ppm for H_b, 0.47 ppm for H_c, respectively) due to the shielding effects inside the electron-rich cavity of pillar[5]arene unit. The rotation of the diamine ring would be limited robustly through the amidation reaction. As a result, the signals of H_a, H_b, and H_c differed and split into two parts in Fig. 1c. Meanwhile, proton signals H_a and H_b exhibited upfield shifts ($\Delta\delta = 2.74$ ppm for H_a and 0.79 ppm for H_b, respectively), while H_c displayed a downfield shift ($\Delta\delta = 0.05$ ppm) due to the deshielding effect from 5 neighbor oxygen atoms. When **G1** was added to the solution of **MUJ3**, its proton (H_1 and H_2) signals shifted upfield by 2.65 and 3.29 ppm, respectively (Figs. 1d and e), indicating the encapsulation process between **MUJ3** and **G1**. Namely, the inside ring rolled out from the pillar[5]arene cavity.

Moreover, 2D NOESY NMR correlations, using **MUJ2** as an example, obviously revealed NOE signals between protons of NH (−2.93 ppm), $H_{1,1'}$ (2.37 and 1.90 ppm) and $H_{2,2'}$ (−0.07 and −0.19 ppm) on the side ring and pillar[5]arene aromatic protons H_{Ar} (7.0 ppm) in Fig. 2. Similar ^{1}H NMR phenomena and NOE correlations were also observed for other three MUJs (Figs. S18-S20 in Supporting information). These spectral results supported that the self-entrapped conformations dominated under the experimental conditions.

The self-included structures of **MUJ1**, **MUJ2** and **MUJ3** were unambiguously established by X-ray crystallographic analyses (Fig. 3). In their crystal structures (CCDC No. 1856794, 2034235, and

2080798), it was evident that those side rings, consisting of alkyl, NH-containing, or O-containing chains, respectively, resided within the pillar[5]arene's cavity. Hydrogen bonds formed between the amide NH groups and two oxygen atoms on the modified phenyl unit should contribute greatly to the formation of the self-threaded structure (Figs. S21-S23 in Supporting information). Moreover, the fused side ring was also stabilized within the pillar[5]arene cavity through multiple CH/π interactions, which was proved to be existed in other aromatic hydrocarbons [46]. Previous reports have indicated that the length of the C4-containing alkyl chain could be well-suited to the pillar[5]arene cavity, and therefore, **MUJ2** was expected to have structural stability and rigidity [47]. On the other hand, the other three MUJs may exhibit relatively weakened stability but strong flexibility, offering the potential for manipulating chiroptical inversion.

To study the rolling in/out properties of the side rings on the MUJs, ^{1}H NMR titration experiments were conducted in $CDCl_3$ upon the addition of an excess amount of competitor 1,4-dicyanobutane (**G1**), known for its strong binding affinity towards pillar[5]arene derivatives [48]. Upon the addition of **G1** to **MUJ1**, **MUJ3**, and **MUJ4**, partial proton signals of **G1** shifted upfield at −0.20 and −1.45 ppm, demonstrating a shielding effect of the pillar[5]arene cavity due to the encapsulation of **G1** (Figs. S24-S26 in Supporting information). In contrast, **MUJ2** showed only slight ^{1}H NMR spectral changes under similar conditions, presumably due to its more stable self-inclusion structure (Fig. S27 in Supporting information). This implies that **G1** was not able to effectively push the NH-containing inside ring out of the cavity due to the fitted length of the side ring and the structural rigidity of **MUJ2**. These titration results are consistent with the conclusions drawn from single crystal analysis.

All above NMR spectral findings encouraged us to resolve MUJs racemic mixtures for investigating the possible chiroptical inversion behavior. Enantiomer pairs of MUJs were successfully separated with chiral HPLC using appropriate mobile phases, and each MUJ gave two fractions labeled as f1 and f2, respectively, corresponding a pair of enantiomers of MUJs (Fig. S28 in Supporting information). Circular dichroism (CD) spectra of MUJs' f1 displayed a positive Cotton effect at $\lambda_{ext} = 310$ nm except for **MUJ2**, which exhibited a negative effect, while the CD spectra of f2 showed a mirror-image Cotton effect. Based on our previous report, we can conclude that the fraction with the positive Cotton effect corresponds to the *in-pR* configuration, while the counter-fraction corresponds to the *in-p*S configuration [32]. Furthermore, the supramolecular circular polarized luminescent (CPL) [49] response behavior of MUJs was studied in the absence and presence of **G1** (Fig. 4). For example, two fractions of **MUJ3** displayed mirror-imaged CPL emissions, giving positive CPL for **MUJ3**-f1 and negative CPL for **MUJ3**-f2 peaked *ca.* 320 nm. Upon the addition of **G1**, CPL signals weakened significantly as a result of the formation of the complex of **G1⊂MUJ3**, showing an efficient manipulation of CPL by supramolecular complexation.

Next, we focused on investigating the chiroptical inversion behaviors of the f1 of MUJs in response to solvent, temperature, and guest effects. The CD extremum (CD_{ex}) of **MUJ1**-f1 and **MUJ3**-f1 showed no significant changes in the selected solvents (Fig. S29 in Supporting information), suggesting no solvent-dependent chiroptical switching. Subsequently, the effects of temperature were examined by varying the temperature from 5 °C to 60 °C in $CHCl_3$ and CH_3OH (Fig. S30 in Supporting information). For all MUJs, temperature variation only caused a slight decrease in CDex without inducing chiroptical inversion.

To perform guest-triggered chiroptical inversion, titration experiments of enantiomer f1 upon the addition of **G1** were carried out by monitoring CD spectral changes in $CHCl_3$ or in CH_3OH. When **G1** was gradually added, **MUJ1**-f1 and **MUJ4**-f1 displayed significant decreases but without chiroptical inversion in $CHCl_3$ (Figs. S31a and d in Supporting information), which suggested only partial side ring rolling out of the cavity. Interestingly, **MUJ3**-f1 underwent a positive-to-negative transformation (Fig. 5a), indicating an inversion of chirality from *in-p*R to *out-p*S. In contrast, **MUJ2**-f1 showed no negative CD_{ex} changes due to its robust self-included structure (Fig. S31b in Supporting information).

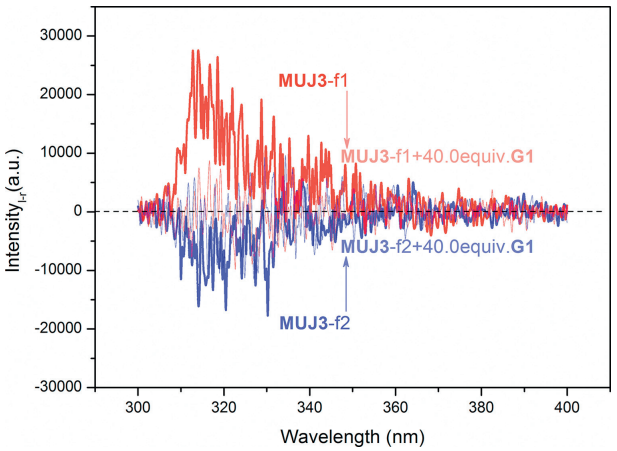

Fig. 4. CPL spectra of two fractions of **MUJ3** (0.01 mmol/L) with **G1** in acetonitrile at 25 °C.

Alternatively, **G1**-triggered chiral inversions were tested in CH_3OH (Figs. 5c and d, Fig. S32 in Suppporting information). Upon addition of **G1**, the positive CD Cotton effect was gradually reduced and inverted to negative ones for **MUJ1**-f1, **MUJ3**-f1, and **MUJ4**-f1 except for **MUJ2**-f1 which demonstrated a medium reduction due to only partial inversion. In the case of the CD titration of **MUJ2**-f1, the solvation of the NH-containing side ring by CH_3OH molecules might account for distinctive spectral changes in $CHCl_3$ and in CH_3OH. In comparison with a robust conformation of methoxy–pill[5]arene self-locked structures reported by Liu and co-workers [42], **MUJ1** displayed de-threaded inversion in CH_3OH, which might be attributed to the hydrogen bonding and solvation effect between the amide side ring and CH_3OH solvent. As shown in Fig. 6, such **G1**-driven planar chirality inversions from *in*-form to *out*-form were observed in both two solutions. The f1 fractions for **MUJ3** in $CHCl_3$, **MUJ1** and **MUJ4** in CH_3OH presented a change of dissymmetric factor g ($g = \Delta\varepsilon/\varepsilon$, where ε is the molar extinction coefficient at a particular wavelength) from positive to negative. These results suggest that solvation plays a dominant role in controlling **G1**-driven chiroptical inversion of the bicyclic pillar[5]arene-type compounds.

Based on CD spectral changes, association constants (K_a) of MUJs with **G1** were calculated by a nonlinear curve fitting method, as shown in the insets of Figs. S31 and S32 (Supporting information). The K_a and corresponding Gibbs free energy change ΔG data were listed in Table 1. Compared with other reported pillar[5]arene analogs [20], MUJs showed extremely lower affinities towards **G1**. This could be attributed to the rotational and motional freedom of

Table 1
Association constants for 1:1 complexation of enantiomer f1 with **G1** determined by CD titrations at 25 °C.

Enantiomers	K (L/mol)[a]	ΔG (kJ/mol) [a]	K (L/mol)[b]	ΔG (kJ/mol)[b]
MUJ1-f1	0.89	0.29	4.86	−3.92
MUJ2-f1	ND	ND	0.80	0.55
MUJ3-f1	2.71	−2.47	7.28	−4.92
MUJ4-f1	0.37	2.46	5.13	−4.05

[a] Measurements were performed at 310 nm in $CHCl_3$.
[b] Measurements were performed at 310 nm in CH_3OH. ND = not determined.

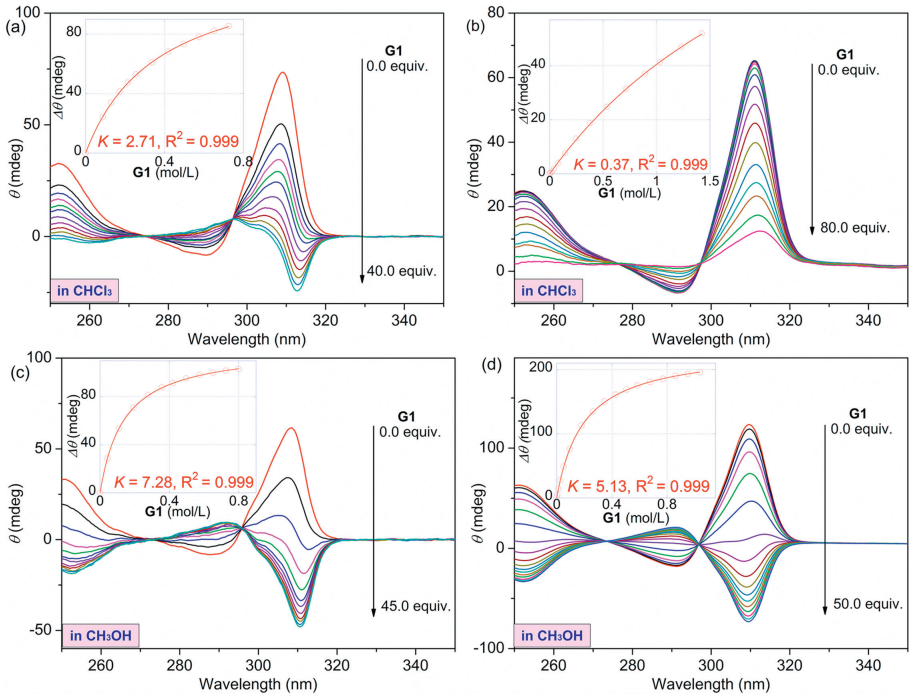

Fig. 5. CD spectral changes of MUJs (0.02 mmol/L, 25 °C) upon addition of **G1** in $CHCl_3$: (a) **MUJ3-f1**, (b) **MUJ4-f1** and in CH_3OH: (c) **MUJ3-f1**, (d) **MUJ4-f1**. Inset: nonlinear fitting curves as a function of the concentration of **G1** at 310 nm.

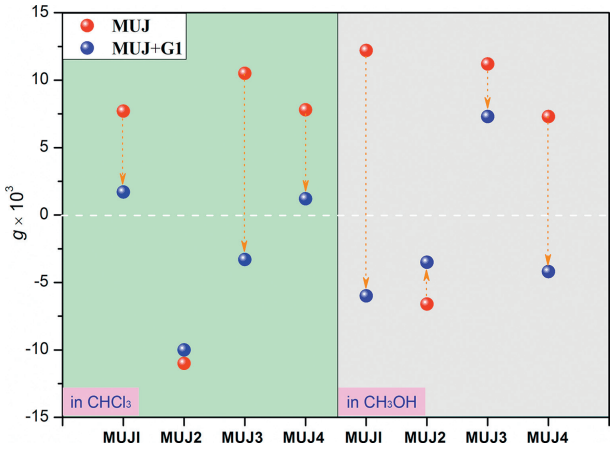

Fig. 6. Extremum changes of the anisotropy factor (g) of **MUJ-f1** enantiomers (0.02 mmol/L, 25 °C) before and after the addition of **G1** at 310 nm in $CHCl_3$ and in CH_3OH.

both pillar[5]arene units and the side ring, which undermines the strength of **G1**. Moreover, it was found that MUJs exhibited higher affinities towards **G1** in CH_3OH than in $CHCl_3$. This could be due to the availability of the pillar[5]arene cavity for accommodating **G1** or CH_3OH molecules and the easy solvation on the side ring by CH_3OH through additional hydrogen bonds between N, O, or S-heteroatomic groups and solvent molecules. Meanwhile, **G1** was captured in the cavity by multiple CH/π, CH/O, and CH/N interactions. To accomplish the chirality inversion, the inside ring must be expelled from the cavity, facilitated by the insertion of **G1** and solvation of the inside-out ring (Fig. 7). Besides, **G1**-driven handedness switching was observed for **MUJ3**-f1 in both solvents along with the largest association constants. This could be attributed to the higher solvation of ethylene glycol side chains relative to other side rings, which furthermore promotes the chiral inversion and stabilization of the out-conformational host-guest complex.

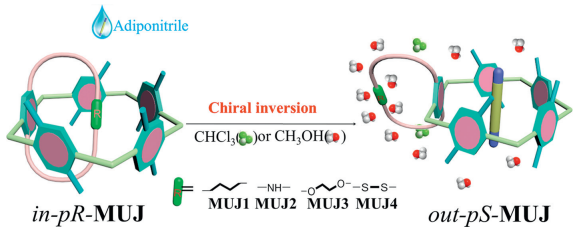

Fig. 7. Cartoon representation for chirality inversion of pseudo[1]catenanes.

In summary, we designed and synthesized four novel pseudo[1]catenane-type pillar[5]arene-based MUJs fusing by a N, O, or S-containing sider ring, whose self-inclusion structures were confirmed by NMR spectra and single crystal analyses. It was found that **G1** could thread into the cavity of **MUJ1**, **MUJ3**, and **MUJ4**, except **MUJ2**, which exhibited strong structural stability and rigidity. No **G1**-triggered chirality switching of **MUJ2**-f1 was observed in $CHCl_3$ and in CH_3OH, whereas **MUJ3**-f1 bearing one oxyethylene unit exhibited significant chiroptical inversion along with positive-to-negative CD spectra changes. The self-included interactions and the solvation on the side ring played important roles in controlling the chiroptical inversion of the pillar[5]arene moiety. Further work will focus on exploring chiroptical inversion driven by other stimuli, such as metal ions, acids/bases, and reductants/oxidants of disulfide bonds. These findings provide valuable insights into the dynamic behavior of pillar[5]arene derivatives and their potential applications in supramolecular chemistry and molecular machines.

Declaration of competing interest

The authors declare that they have no known competing financial interests or personal relationships that could have appeared to influence the work reported in this paper.

Acknowledgments

We acknowledge the support of this work by the National Natural Science Foundation of China (Nos. 92056116, 21871194, 21971169), National Key Research and Development Program of China (No. 2017YFA0505903).

Supplementary materials

Supplementary material associated with this article can be found, in the online version, at doi:10.1016/j.cclet.2023.108757.

References

[1] L. Zhang, L. Qin, X. Wang, H. Cao, M. Liu, Adv. Mater. 26 (2015) 6959–6964.
[2] S. Sun, Y. Yang, D. Li, J. Zhu, J. Am. Chem. Soc. 141 (2019) 19524–19528.
[3] L. Yao, K. Fu, X. Wang, et al., ACS. Nano 17 (2023) 2159–2169.
[4] P. Xing, Y. Li, Y. Wang, et al., Angew. Chem. Int. Ed. 57 (2018) 7774–7779.
[5] C. Shi, H. Li, X. Shi, L. Zhao, H. Qiu, Chin. Chem. Lett. 33 (2022) 3613–3622.
[6] F. Mamiya, N. Ousaka, E. Yashima, Angew. Chem. Int. Ed. 54 (2015) 14442–14446.
[7] Y. Nagata, T. Yamada, T. Adachi, et al., J. Am. Chem. Soc. 135 (2013) 10104–10113.
[8] H.K. Bisoyi, Q. Li, Angew. Chem. Int. Ed. 55 (2016) 2994–3010.
[9] J. Kim, J. Lee, W.Y. Kim, et al., Nat. Commun. 6 (2015) 6959–6964.
[10] M. Liu, L. Zhang, T. Wang, Chem. Rev. 115 (2015) 7304–7397.
[11] H. Liang, B. Hua, F. Xu, et al., J. Am. Chem. Soc. 142 (2020) 19772–19778.
[12] R. Lin, H. Zhang, S. Li, et al., Chem. Eur. J. 17 (2011) 2420–2427.
[13] J. Gregolinski, M. Hikita, T. Sakamoto, et al., Inorg. Chem. 55 (2016) 633–643.
[14] E. Ohta, H. Sato, S. Ando, et al., Nat. Chem. 3 (2011) 68–73.
[15] J. Suk, V.R. Naidu, X. Liu, M.S. Lah, K.S. Jeong, J. Am. Chem. Soc. 133 (2011) 13938–13941.
[16] T. Ogoshi, D. Yamafuji, T. Akutsu, M. Naito, T.A. Yamagishi, Chem. Commun. 49 (2013) 8782–8784.
[17] E. Lee, H. Ju, I.H. Park, et al., J. Am. Chem. Soc. 140 (2018) 9669–9677.
[18] K. Kato, S. Fa, S. Ohtani, et al., Chem. Soc. Rev. 51 (2022) 3648–3687.
[19] F. Gao, X. Yu, L. Liu, et al., Chin. Chem. Lett. 34 (2023) 107558–107561.
[20] T. Ogoshi, T. Yamagishi, Y. Nakamoto, Chem. Rev. 116 (2015) 7937–8002.
[21] S. Fa, T. Kakuta, T. Yamagishi, T. Ogoshi, Chem. Let. 48 (2019) 1278–1287.
[22] A. Imayoshi, B.V. Lakshmi, Y. Ueda, T. Yoshimura, T. Kawabata, Nat. Commun. 12 (2021) 404.
[23] J. Ye, L. Li, Y. You, et al., J. Am. Chem. Soc. 145 (2023) 384–390.
[24] H. Zhang, Z. Liu, F. Xin, Y. Zhao, Coord. Chem. Rev. 420 (2020) 213425–213433.
[25] C. Yan, Z. Zhang, Y. Ding, et al., Chin. Chem. Lett. 32 (2021) 1267–1279.
[26] S. Yu, Y. Wang, S. Chatterjee, et al., Chin. Chem. Lett 32 (2021) 179–183.
[27] L. Wu, C. Han, X. Jing, Y. Yao, Chin. Chem. Lett. 32 (2021) 3322–3330.
[28] F. Lu, Y. Chen, B. Fu, S. Chen, L. Wang, Chin. Chem. Lett. 33 (2022) 5111–5115.
[29] C. Liu, L. Zhou, S. Guo, H. Zhang, J. Han, Polym. Chem. 13 (2022) 286–299.
[30] K. Wang, X. Tian, J.H. Jordan, et al., Chin. Chem. Lett. 33 (2022) 89–96.
[31] H. Qiang, T. Chen, Z. Wang, et al., Chin. Chem. Lett. 31 (2020) 3225–3229.
[32] J. Yao, W. Wu, W. Liang, Y. Feng, C. Yang, Angew. Chem. Int. Ed. 129 (2017) 6869–6873.
[33] S. Fa, K. Adachi, Y. Nagata, et al., Chem. Sci. 12 (2021) 3483–3488.
[34] X. Yu, W. Wu, D. Zhou, et al., CCS Chem 4 (2022) 1806–1814.
[35] Y. Zhou, G. Zhuang, P. Du, Chin. Chem. Lett. 34 (2023) 108593.
[36] D. Zhang, W. Liang, J. Yi, et al., Sci. China Chem. 65 (2022) 1149–1156.
[37] J. Yao, W. Wu, C. Xiao, et al., Nat. Commun. 12 (2021) 2600.
[38] J. Yao, H. Mizuno, C. Xiao, et al., Chem. Sci. 12 (2021) 4361–4366.
[39] C. Fan, J. Yao, G. Li, et al., Chem. Eur. J. 25 (2019) 12526–12537.
[40] C. Xiao, W. Wu, W. Liang, et al., Angew. Chem., Int. Ed. 59 (2020) 8094–8098.
[41] Y. Lv, C. Xiao, C. Yang, New. J. Chem. 42 (2018) 19357–19359.
[42] S.H. Li, H.Y. Zhang, X. Xu, Y. Liu, Nat. Commun. 6 (2015) 7590–7596.
[43] G. Yu, B. Hua, C. Han, Org. Lett. 16 (2014) 2486–2489.
[44] N.L. Strutt, R.S. Forgan, J.M. Spruell, Y.Y. Botros, J.F. Stoddart, J. Am. Chem. Soc. 133 (2011) 5668–5671.
[45] L. Shao, Y. Pan, B. Hua, et al., Angew. Chem., Int. Ed. 59 (2020) 11779–11783.
[46] G. Huang, W. Liu, A. Valkonen, et al., Chin. Chem. Lett. 29 (2018) 91–94.
[47] C. Li, Q. Xu, J. Li, F. Yao, X. Jia, Org. Biomol. Chem. 8 (2010) 1568–1576.
[48] X. Shu, S. Chen, J. Li, et al., Chem. Commun. 48 (2012) 2967–2969.
[49] C. Tu, W. Wu, W. Liang, et al., Angew. Chem. Int. Ed. 61 (2022) e202203541.